Short article

Diverse Gut Pathogens Exploit the Host Engulfment Pathway via a Conserved Mechanism

AUTHORS:
Mahitha Shree Anandachar[1,2], Agyekum Boadi[1], Saptarshi Sinha[1], Suchismita Roy[1], Stella-Rita Ibeawuchi[2], Hobie Gementera[2], Alicia Amamoto[2], Gajanan D. Katkar[1‡] and Pradipta Ghosh[1, 3‡*]

AFFILIATIONS:
[1]*Department of Cellular and Molecular Medicine, University of California San Diego.*
[2]*Department of Pathology, University of California San Diego.*
[3]*Department of Medicine, University of California San Diego.*

*Lead Contact

‡CORRESPONDING AUTHORS:

Gajanan D. Katkar, Ph.D.; Departments of Cellular and Molecular Medicine, University of California San Diego, CA 92093. **Phone**: 858-346-3507: **Email:** kgajanandattatray@ucsd.edu

Pradipta Ghosh, M.D.; Professor, Departments of Medicine and Cellular and Molecular Medicine, University of California San Diego, CA 92093. **Phone**: 858-822-7633: **Email:** prghosh@ucsd.edu

ABSTRACT

Macrophages clear infections by engulfing and digesting pathogens within phagolysosomes. Pathogens escape this fate by engaging in a molecular arms race; they use *WxxxE* motif-containing "effector" proteins to subvert the host cells they invade and seek refuge within protective vacuoles. Here we define the host component of the molecular arms race as an evolutionarily conserved polar 'hotspot' on the PH-domain of ELMO1 (*E*ngu*l*fment and Cell *Mo*tility1), which is targeted by diverse *WxxxE*-effectors. Using homology modeling and site-directed mutagenesis, we show that a lysine triad within the 'patch' directly binds all *WxxxE*-effectors tested: SifA (*Salmonella)*, IpgB1 and IpgB2 (*Shigella*), and Map (enteropathogenic *E. coli*). Using an integrated SifA•host protein-protein interaction (PPI) network, *in-silico* network perturbation, and functional studies we show that the major consequences of preventing SifA•ELMO1 interaction are reduced Rac1 activity and microbial invasion. That multiple effectors, all diverse in structure, function, and sequence bind the same hotpot on ELMO1 suggests that the *WxxxE*-effector(s)•ELMO1 interface is a convergence point of intrusion detection and/or host vulnerability. We conclude that the interface may represent the fault line in co-evolved molecular adaptations between pathogens and the host and its disruption may serve as a therapeutic strategy.

KEY WORDS:

ELMO1, Rac1, Dock180, *SifA, Engulfment, Salmonella, WxxxE*-motif

GRAPHICAL ABSTRACT

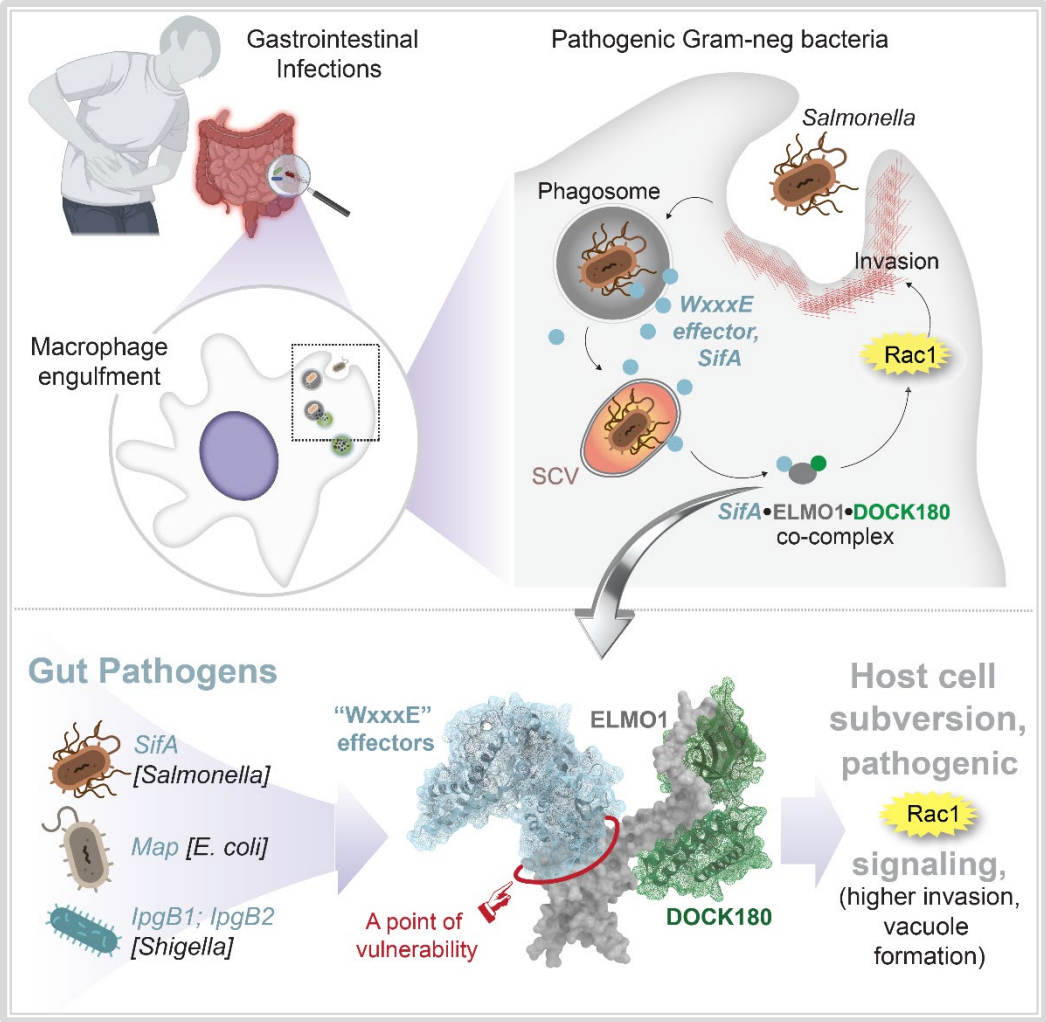

In brief:
This work defines the nature of a conserved molecular interface, assembled between diverse W*xxxE* motif-containing effector proteins encoded by gut pathogens and the host innate immune sensor, ELMO1, via which pathogens exploit the host's engulfment machinery.

HIGHLIGHTS

- Gut pathogens trick macrophages to enter and form vacuoles of refuge within the host.
- Diverse pathogens use *WxxxE* motif-containing effectors to bind a conserved surface on ELMO1.
- *WxxxE*-effector•ELMO1 interaction activates Rac1 and promotes bacterial invasion.
- Disrupting the *WxxxE*-effector•ELMO1 interface may serve as a therapeutic strategy.

INTRODUCTION

Enteric pathogens such as *Salmonella* rely upon their virulence factors to invade and replicate within host cells. Upon invasion, they seek refuge within a modified phagosome-like structure, the *Salmonella*-containing vacuole (SCV)[1], within which they survive, even replicate, or simply persist in a dormant-like state[2]. Both invasion and SCV formation require the delivery of microbial effector proteins via Type III Secretion Systems (T3SSs) into the host cell; they both require the cooperation of a subverted host cell whose phagolysosomal signaling and membrane trafficking pathways are manipulated to mount very dynamic and extensive membrane remodeling and actin rearrangement[1]. Thus, three key aspects facilitating *Salmonella* pathogenesis are (i) vacuole formation for refuge, (ii) delivery of effector proteins via T3SSs to interfere and/or manipulate the host system, facilitating (iii) more bacterial invasion. These mechanisms of pathogenesis are shared also among other enteric pathogens such as enteropathogenic *E. coli* EHECs, EPECs, and *Shigella*. *E. coli* rely upon T3SS effectors--e.g., Map, EspH, and EspF--to form *E. coli*-containing vacuoles (ECVs)[3] and manipulate the host cell form pedestals[4], filopodia, or microspikes for invasion, whereas *Shigella* rely upon T3SS effectors, e.g., IpgB1/2, to form vacuoles[5] and manipulate host cells into forming membrane ruffles for orchestrating what is known as "the trigger mechanism of entry"[6-9]. Similar mechanisms are also used by *Yersinia*[10] and *Campylobacter*[11] to subvert host epithelial cells.

Regardless of the diversity of the pathogens, their equally diverse T3SS injectosomes, or the repertoire of effectors (reviewed in[12]), the host actin cytoskeleton has emerged as the dynamic hub in a microbe-induced circuitry of Ras-superfamily GTPases [Ras homolog family member A (RhoA), Ras-related C3 botulinum toxin substrate 1 (Rac1) and Cell division control (Cdc) protein-42][13]. Diverse microbes converge upon and exploit this host circuitry to mount pathogenic signaling, escape lysosomal clearance by seeking refuge in vacuoles, invade host cells and alter inflammatory response. As for mechanism(s) for such convergence, the ability of a *WxxxE* motif-containing family of effectors to directly activate host GTPases was reported first[14]. Engulfment and cell Motility protein 1 (ELMO1) was identified subsequently as a *WxxxE* effector-interacting host protein[15]. Three independent groups, each using ELMO1-knockout animals that were infected with different pathogens (*Shigella*[6], *Salmonella*[15]and *E. coli*[16]), have implicated the *WxxxE*•ELMO1 interaction in the augmentation of the actin•GTPase circuitry via the well-established ELMO1•DOCK180 (Dedicator of cytokinesis)→Rac1 axis[17-19]. Within this signaling cascade, ELMO1•Dock180 is a bipartite guanine nucleotide exchange factor (GEF) for the monomeric GTPase Rac1.

Despite these insights, the basis for how functionally diverse *WxxxE* motif-containing effectors may bind ELMO1 and induce convergent pathogenic signaling via the ELMO1•DOCK•Rac1 axis remains unknown. Using a transdisciplinary and multi-scale approach that spans structural models as well as protein-protein interaction networks, here we reveal a surprisingly conserved molecular mechanism for how diverse pathogens use their *WxxxE*-effectors to hijack the ELMO1•DOCK•Rac1 axis via a singular point of vulnerability on ELMO1.

RESULTS AND DISCUSSION

ELMO1 and SifA *cooperate during vacuole formation.*

Prior work has separately implicated both ELMO1[20] and SifA[21-23] in *Salmonella* pathogenesis. While SifA has been directly implicated in the formation of SCVs[22,23], ELMO1 was shown to impact bacterial colonization, dissemination, and inflammatory cytokines *in vivo*[15]. We asked if both proteins are required for SCV formation. We stably depleted ELMO1 in J774 macrophages by short hairpin (sh)RNA (>99% depletion compared to controls; **Figure 1A**), infected them with either the WT (SL) or a mutant *Salmonella* strain that lacks *SifA* (*ΔSifA*), and then assessed the ultrastructure of the SCVs by transmission electron microscopy (TEM) (see workflow; **Figure 1B**). Bacteria were observed as either intact within vacuoles, free in cytosol, or partially digested within fused lytic compartments, as reported previously[24] (**Figure 1C-D**). When assessed for the completeness of the vacuolar wall (see basis for quantification; **Figure 1E**), WT *Salmonella* formed complete SCVs at a significantly lower rate in ELMO-depleted macrophages compared to controls (13% vs 35%; **Figure 1F, H**). Absence of SifA impaired SCV biogenesis regardless of the presence or absence of ELMO1 (**Figure 1G, H**). Findings demonstrate that both ELMO1 and SifA are required for SCV formation and suggest cooperativity between the two proteins during SCV biogenesis.

SifA *directly binds the C-terminus of ELMO1.*

We next asked if SifA binds ELMO1; the latter is a multi-modular protein with several known interacting partners (summarized in **Figure 1I**). We compared head-to-head equimolar amounts of GST-tagged full length vs. a C-terminal fragment (aa 482-727) of ELMO1 [which contains a pleckstrin-like homology domain (PHD)-; **Figure 1I**] for their ability of to bind a His-tagged recombinant SifA protein. The C-terminal PH-domain was prioritized because of two reasons: (i) A recent domain mapping effort using fragments of ELMO1 on cell lysates expressing SifA had ruled out contributions of the N-terminal domain in mediating this interaction[15]; and (ii) SifA directly binds another PH-domain, SKIP, forming 1:1 complex at micromolar dissociation constant, the structural basis for which has been resolved[25,26]. We found that both full length ELMO1 and its C-terminal fragment can bind His-SifA (**Figure 1J**). Binding was also observed when the bait and prey proteins were swapped, such that immobilized GST-SifA was tested for its ability to bind His-ELMO1 proteins (**Figure 1K**). Because interactions occurred between recombinant proteins purified to >95% purity, we conclude that the SifA•ELMO1 interaction is direct. Because SifA bound both the full length and the C-terminal fragment of ELMO1 to a similar extent, we conclude that the C-terminus of ELMO1 is sufficient for the interaction.

SifA *binds to an evolutionarily conserved lysine hotspot on ELMO1's PH domain.*

To gain insights into the nature of the SifA•ELMO1 interface, we leveraged two previously resolved structures of a SifA•SKIP-PHD co-complex[23] and ELMO1-PHD to build a homology model of SifA•ELMO1-PHD co-complex (see *Methods*). The resultant model helped draw three key important conclusions: (i) the resolved structure of SifA•SKIP[23] and the model for SifA•ELMO1 (**Figure 2A**) were very similar, and hence, the specific recognition of SifA by both SKIP-PHD and ELMO1-PHD was predicted to be mediated through a

large network of hydrogen(H)-bonds and van der Waals contacts; (ii) the tryptophan (W197, deeply buried within the hydrophobic core of SifA) and glutamate (E201) within the *WxxxE*-motif (red residues; **Figure 2A**), which are essential for the stability and the translocation of SifA, but proven to be dispensable for binding SKIP[26] (**Figure 2A**) are likely to be nonessential also for ELMO1; and (iii) the amino acids deemed essential for the assembly of the SifA•ELMO1 interface were: a pair of hydrophobic residues, Leucine (L)130 and Methionine (M)131 on SifA (blue; **Figure 2B**) and a triad of polar lysine residues within the β3-β4 loop of ELMO1 (K620, K626 and K628) (red; **Figure 2B**). An alignment of the sequences of ELMO1-PHD and SKIP-PHD showed the lysine triad in ELMO1 corresponds to the corresponding contact sites on SKIP for SifA in the resolved co-complex[26] (**Figure 2C, S1A**). We noted that K621 is reported to be ubiquitinated and the Threonine (T) at 619 is phosphorylated (**Figure S1B**); none of the lysine residues are reported to be impacted by germline SNPs or somatic mutations in cancers. Most importantly, the lysine triad in ELMO1 is evolutionarily conserved from fish to humans, as well as in the homologous members of the family, ELMO2 and ELMO3 (**Figure 2D**; **S2**).

We validated the homology model by generating several structure-rationalized mutants. The positively charged lysines on ELMO1 were substituted with negatively charged aspartate residues (D; ELMO1-CT-K3D). Similarly, each hydrophobic residue, L130 and M131 on SifA was substituted with an unfavorable negatively charged and polar aspartate residue, either alone (L130D; M131D) or in combination (LM>DD). Binding to SifA was significantly reduced in the case of the K3D ELMO1 mutant (**Figure 2E-F**), and binding to ELMO1 was virtually abolished in the case of all the SifA mutants (**Figure 2G**). Strong polar contacts between L130(SifA) and the lysine triad (ELMO1) were predicted as critical for the SifA•ELMO1 interaction (**Figure 2H**). We confirmed the relative contributions of these residues in pulldown assays which showed that SifA•ELMO1 interactions were partially impaired when L130D-SifA and K3D-ELMO1 substitutions when used alone (**Figure 2I-J**) and virtually lost when the mutants were used concomitantly (**Figure 2I-J**).

These findings provide atomic level insights into the nature and composition of the SifA•ELMO1 complex which is assembled when a pair of hydrophobic residues on SifA binds an evolutionarily conserved polar hot spot on ELMO1-PHD. Strong hydrophobic interactions stabilize the SifA•ELMO1 interface which can be selectively disrupted.

Disrupting the SifA•ELMO1 interface suppresses Rac1 activity and bacterial invasion.

To assess the impact of selective disruption of the SifA•ELMO1 interface in the setting of an infection, we used an unbiased network-based approach. We leveraged a previously published[27] SifA interactome, as determined by proximity-dependent biotin labelling (BioID) and used those interactors as 'seeds' for fetching additional interactors to build an integrated SifA(*Salmonella*)•host PPI network (see *Methods* for details). The resultant network (**Figure S3A**) was perturbed by *in-silico* deletion of either ELMO1 (**Figure 3A, S3B**) or, more specifically, the SifA•ELMO1 interaction (**Figure 3B**). Both modes of perturbation were analyzed by a differential network analysis (with *vs*. without perturbations) using various network metrices (see legends; **Figure 3C, E**). As one would expect, deletion of ELMO1 impacts many proteins (**Figure 3C**; **S3C-D**), including those engaged in microbe sensing (BAI1, NOD1, NOD2), membrane trafficking along the phagolysosomal

pathway (EEA1, Rab5A, Rab9A and LAMP), multiple Src-family kinases (LYN, YES and HCK), inflammatory cytokines (IL1B, CCL2/MCP1, CXCL12, and TNF), as well as immune cell (B cell) and epithelial (adherens junction) pathways (**Figure 3D**). Findings are consistent with prior published work, implicating ELMO1 in facilitating the recruitment of LAMP1 to SCVs[28], mounting a cytokine response[15,20], as well as regulating epithelial junctions[29] upon *Salmonella* infection. The proteins found to be impacted based on at least two network metrices (**Figure 3C**) are enriched for Rac1 signaling (Rac1, Rac2, Nckap1 and Dok180) and the endolysosomal pathway (LAMP and RABs). The more refined approach of selective deletion of the SifA•ELMO1 interaction yielded, as expected, a smaller list of proteins that mostly concerned with the DOCK1•RAC signaling axis and Src family kinases, HCK, LYN and YES (**Figure 3E-F**). Because phosphorylation of ELMO1 by Src-family kinases such as Src, Fyn[30], and HCK[31] also converge on Rac1 activity, Rac1 signaling, likely via the ELMO1•DOCK1 axis, emerged as the most important function predicted to be impacted in infected cells.

Structure homology models of ternary complexes of SifA•ELMO1•DOCK revealed that although both SifA and DOCK180 bind ELMO1-PHD, they do so via two distinct and non-overlapping interfaces (**Figure 3G**). To experimentally validate this finding, we generated a mutant ELMO1 (W665A) that was previously confirmed by two independent groups to be essential for binding DOCK180[32,33] and tested its ability to bind His-SifA in pulldown assays. Both WT and ELMO1-W665A bound SifA to similar extents, indicating that W665 is dispensable for binding SifA (**Figure 3H**). Findings are also consistent with the fact that both SifA and DOCK180 co-immunoprecipitate with ELMO1[15], and hence, may exist as a ternary complex.

We anticipated that selective disruption of the SifA•ELMO1 interface (using the ELMO1-K3D mutant), while leaving intact the ELMO1•DOCK interface, would interrupt the ELMO1•DOCK•Rac1 signaling axis and reduce bacterial invasion (**Figure 3I-J)**. This was indeed found to be the case as Rac1 signaling was induced during *Salmonella* infection in ELMO1-depleted J774 macrophages reconstituted with WT ELMO1 but found to be significantly blunted when the same macrophages were reconstituted with the K3D mutant ELMO1 (**Figure 3K-L**). Reduced Rac1 activity was also associated with reduced bacterial internalization (**Figure 3M**). Findings demonstrate that one of the major consequences of mutating the polar triad of lysine residues on ELMO1 is reduction in both Rac1 activity and microbial invasion.

Diverse WxxxE-effectors target the same lysine hotspot on ELMO1.

Prior work using ELMO1-*knockout* zebrafish (*E. coli*/MAP[16]) and mouse (*Shigella*/IpgB1[6] and *Salmonella*/*SifA*)[15] have independently concluded that diverse pathogens trigger host immune responses via *WxxxE*•ELMO1 interactions. We asked if our insights into the nature of the SifA•ELMO1 interface are relevant also to other *WxxxE* motif-containing effectors. As observed previously for SifA (**Figure 1J-K**), *WxxxE* effectors IpgB1, IpgB2 and Map also directly bound both full length (**Figure 4A**-*top*) and the C-terminal PHD containing fragment (**Figure 4A**-*bottom*) of ELMO1. More importantly, mutation of the polar lysine triad on ELMO1 reduced the binding of all effectors tested (**Figure 4B-C**), indicating that these effectors require the same hotspot as SifA to engage with ELMO1, presumably via similar hydrophobic contacts. Because the

effectors have little to no sequence similarity other than the invariant *WxxxE*-motif (see alignment; **Figure S4**), and the N-terminal extension is unique to SifA, we were unable to predict the exact nature of the potential hydrophobic contacts on the effectors. We conclude that the newly identified hotspot on ELMO1 represents a point of convergence for numerous *WxxxE*-effectors encoded by diverse pathogens to engage with one host protein. It is noteworthy that each of these *WxxxE*-effectors we tested here, have recently been shown to require ELMO1 for inducing Rac1 signaling[15].

CONCLUSIONS AND STUDY LIMITATIONS

This work provides an atomic-level resolution of a single point of vulnerability within the host engulfment pathway, i.e., a hot spot (lysine triad) on the ELMO1-PHD. This hot spot is exploited by diverse gut pathogens such as *Salmonella* to activate the ELMO1•DOCK180•Rac1 axis, invade host cells and seek refuge within SCVs (see summary of findings; **Figure 4D**). These findings come as a surprise because the bacterial effector proteins that are responsible for such exploitation are diverse, and yet, they all bind the same hot spot on ELMO1 to hijack the Rac1 axis to their advantage (see legend; **Figure 4E**).

Because the *WxxxE* signature motif is found in enteric as well as plant pathogens, and within the Toll/interleukin-1 receptor (TIR) modules of both host and pathogen proteins (but notably absent in commensals[15]), it is possible that some host *WxxxE*-proteins may also engage ELMO1 via the same hot spot. If so, the pathogen-encoded *WxxxE*-effectors should competitively block such interactions, exemplifying the phenomenon of molecular mimicry. The fact that the polar lysine triad at the hot spot on ELMO1 is evolutionarily intact from fish to humans and resembles a similar patch on SKIP's PH domain suggests that these conserved hot spots on host protein surfaces may have co-evolved with the pathogens as part of a molecular arms race of adaptations. The deleterious impact of structure-rationalized mutants suggests that both the SifA•ELMO1 (shown here) and the SifA•SKIP (published before[23,26]) interfaces are sensitive to disruption. This is particularly important because hydrophobic interactions that stabilize protein-protein interfaces via a central cluster of hot spot residues are of high therapeutic value because they are amenable to disruption with rationally designed small molecule inhibitors[34].

This study also has few limitations. For example, how post-translational modifications (PTMs) may impact the *WxxxE*•ELMO1 interface was not evaluated. It is possible that lysine methylation, which ironically was described as a PTM first in *Salmonella* flagellin[35], may impact the interface, as shown in other instances[36]. Similarly, phosphorylation at T619 or ubiquitination at K621 may have impacts that were not explored; because the ELMO1•DOCK180 co-complex is known to be regulated by ubiquitination[37], and both proteins are downregulated rapidly upon LPS stimulation[38], we speculate that ubiquitination at K621 may deter *WxxxE*-effector interactions and thereby, serve as a protective strategy of the host during acute infections. Finally, the impact of disrupting the *WxxxE*•ELMO1 interface on host immune responses were not studied here and will require the creation of knock-in K3D mutant models. All these avenues are expected to provide a more complete picture of the consequences of disrupting the *WxxxE*•ELMO1 interface and help formulate strategies to disrupt it for therapeutic purposes.

In conclusion, our studies characterize a polar patch on ELMO1-PHD as a conserved hot spot of host vulnerability—a so-called Achilles heel--which is exploited by multiple pathogens. Because prior studies on ELMO1-*knockout* zebrafish[16] and mice[6,15] have implicated *WxxxE*•ELMO1 interactions as responsible also for mounting host inflammatory responses, the same polar patch on ELMO1-PHD may also serve as a conserved hot spot of intrusion detection.

FIGURES AND LEGENDS (1304 WORDS)

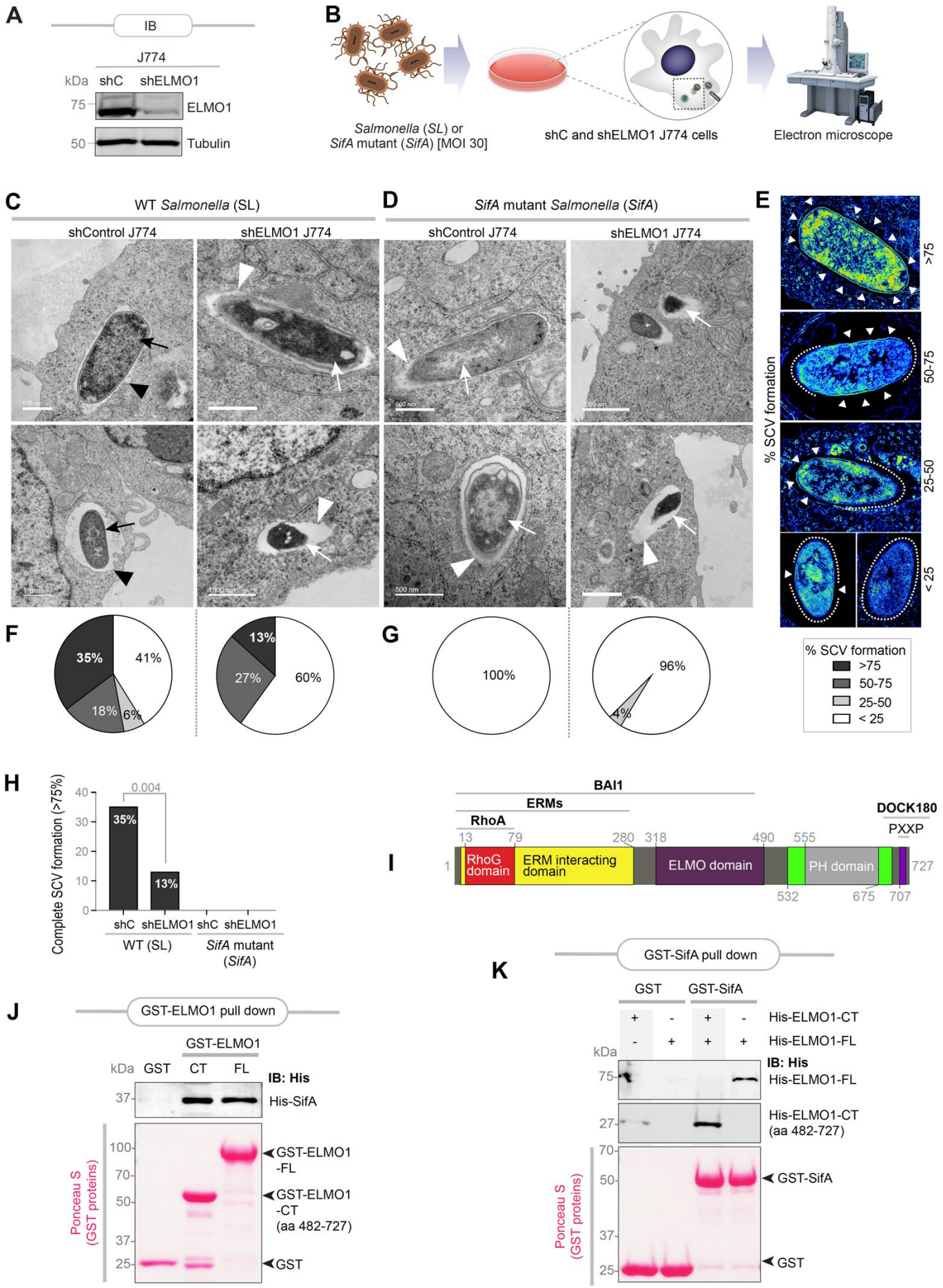

Figure 1: ELMO1 and SifA interact directly and cooperate to promote SCV formation.

A: Immunoblot of control (shC) and ELMO1-depleted (shELMO1) J774 murine macrophages.

B: Schematic shows workflow for TEM on J774 macrophages infected with either *Salmonella* (SL) or a *SifA*-deleted variant strain (SifA) of the same.

C-D: Representative electron micrographs of control (shC) or ELMO1-depleted (shELMO1) J774 macrophages, infected with *S. typhimurium* (SL or *SifA*; 30 moi), at 6 h post-infection. Examples of bacteria within vacuoles (black arrowheads) and cytosolic bacteria (white arrowheads) are indicated. Bacteria that are either Intact (black arrows) or partially degraded upon fusion with lytic compartments (white arrows) are also indicated. Scale bars are placed at the lower left corner of each micrograph.

E-G: A montage (E) of pseudo-colored micrographs of SCVs at various stages of formation is shown. The presence (arrowheads) or absence (interrupted lines) of detectable vacuolar membrane are marked. Pie charts display the percentage of bacteria at each stage of SCV formation (F-G) encountered in C-D.

H: Bar graph display the percentage of complete (representing >75% in E) SCV formation in C-D.

I: A domain map of ELMO1 with major interacting partners. ERM proteins (ezrin, radixin and moesin); PH, pleckstrin homology; BAI1, Brain-specific angiogenesis inhibitor 1 (*ADGRB1*).

J: Recombinant His-SifA (~5 µg) was used in a pulldown assay with immobilized bacterially expressed recombinant GST-tagged full-length (FL) or a C-terminal domain (CT; aa 482-727) of ELMO1 or GST alone (control). Bound SifA was visualized by immunoblot using anti-His (SifA) antibody. GST proteins are visualized by Ponceau S staining.

K: Recombinant His-tagged CT (aa 482-727) or full-length (FL) ELMO1 proteins (~3 µg) were used in a pulldown assay with immobilized bacterially expressed recombinant full-length GST-SifA or GST alone (control). Bound ELMO1 proteins were visualized by immunoblot using anti-His (SifA) antibody. GST proteins are visualized by Ponceau S staining.

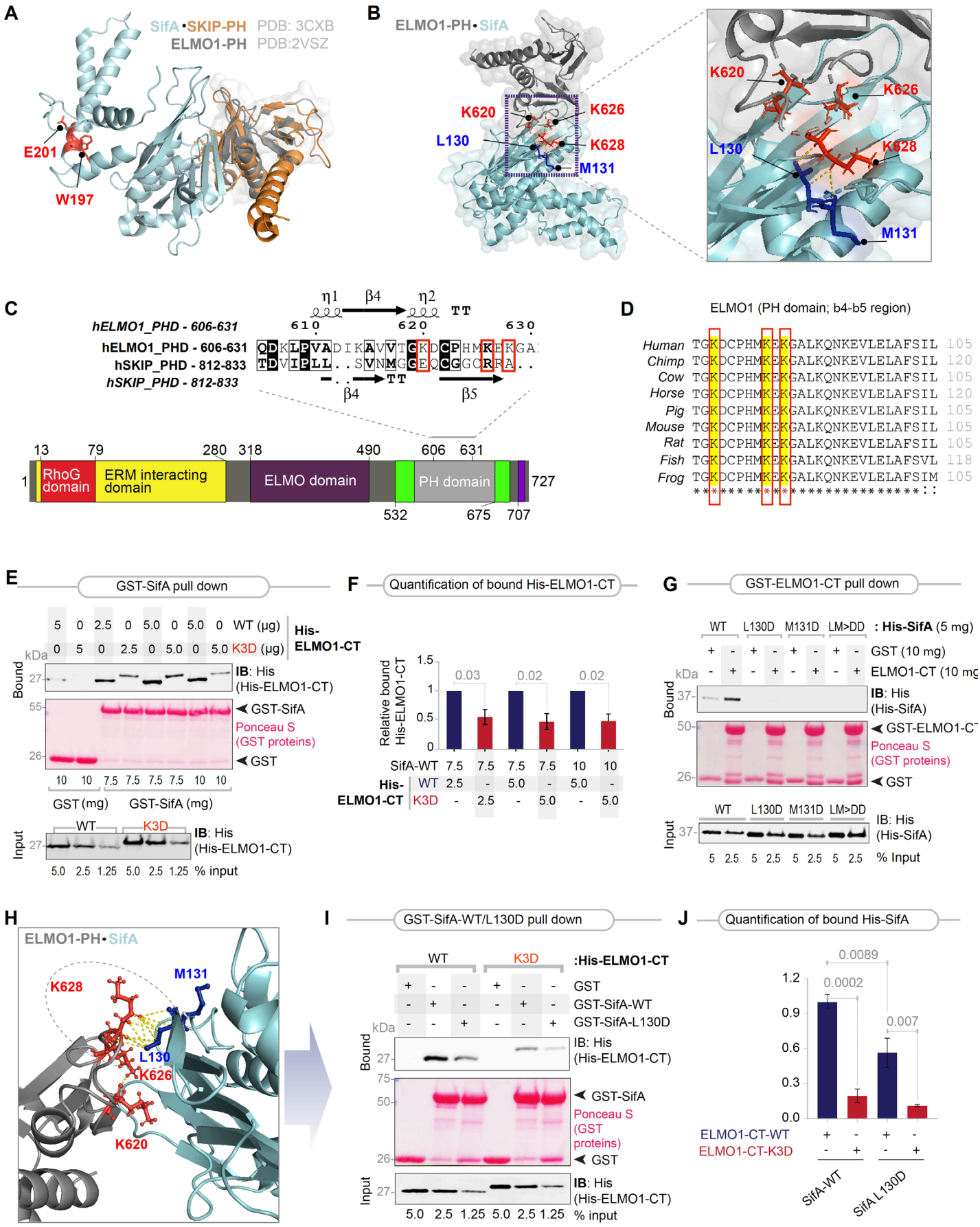

Figure 2: Biochemical characterization of the ELMO1•SifA interface.

A. Homology model of the ELMO1(gray)•SifA(turquoise) complex, generated by superimposing the solved structure of the ELMO1-PH (PDB:2VSZ) on that of the SKIP-PH (golden) in complex with SifA (PDB:3CXB). The executive root mean square deviation (RMSD) of the model is 1.528. The tryptophan (W) and glutamate (E) within the WxxxE-motif in SifA are highlighted in red.

B. *Left*: The homology model in A without SKIP, showing the ELMO1 (gray)•SifA (turquoise) co-complex. Key residues on SifA (royal blue) and ELMO1 (red) that are predicted to form the interface. *Right*: A magnified view of the key residues participating at the ELMO1 (gray)•SifA (turquoise) interface.

C. An alignment of the sequences of the PH domains of ELMO1 and SKIP is shown, along with secondary structures. Conserved residues are shaded in black; similar residues are boxed. Three lysine residues on ELMO1 that correspond to the structurally resolved contact sites of SKIP for SifA are marked with red boxes. See also **Supplementary Figure 1A** for extended alignment.

D. An alignment of ELMO1 showing that the lysine triad highlighted with red box in C is conserved across diverse species. See also **Supplementary Figure 2** for extended alignment.

E. Recombinant WT or K3D mutant His-ELMO1-CT proteins (~2.5 or 5 µg; Input) were used in pulldown assays with immobilized GST alone or GST-SifA (~7.5 or 10 µg). Bound ELMO1 was visualized by immunoblotting using an anti-His (ELMO1) antibody. GST proteins are visualized by Ponceau S staining.

F. Quantification of immunoblots in E. Results are displayed as mean ± S.E.M (n = 3 independent replicates). Statistical significance was determined using an unpaired t-test.

G. Equal aliquots (5 µg; Input) of recombinant His-SifA and its mutants (L130D, M131D, and LM-DD) were used in pulldown assays with immobilized GST alone or GST-ELMO1-CT (10 µg). Bound SifA proteins were visualized by immunoblotting using an anti-His antibody. GST proteins are visualized by Ponceau S staining.

H. Strong polar contacts between L130(SifA) and the lysine triad (ELMO1) are predicted as critical for the SifA•ELMO1 interaction are highlighted.

I. Recombinant WT or K3D mutant His-ELMO1-CT proteins were used in pulldown assays with GST or GST-SifA (WT or L130D mutant). Bound ELMO1 was visualized by immunoblotting using an anti-His antibody. GST proteins are visualized by Ponceau S staining.

J. Quantification of immunoblots in I. Results are displayed as mean ± S.E.M (n = 3 independent replicates). Statistical significance was determined using an unpaired t-test.

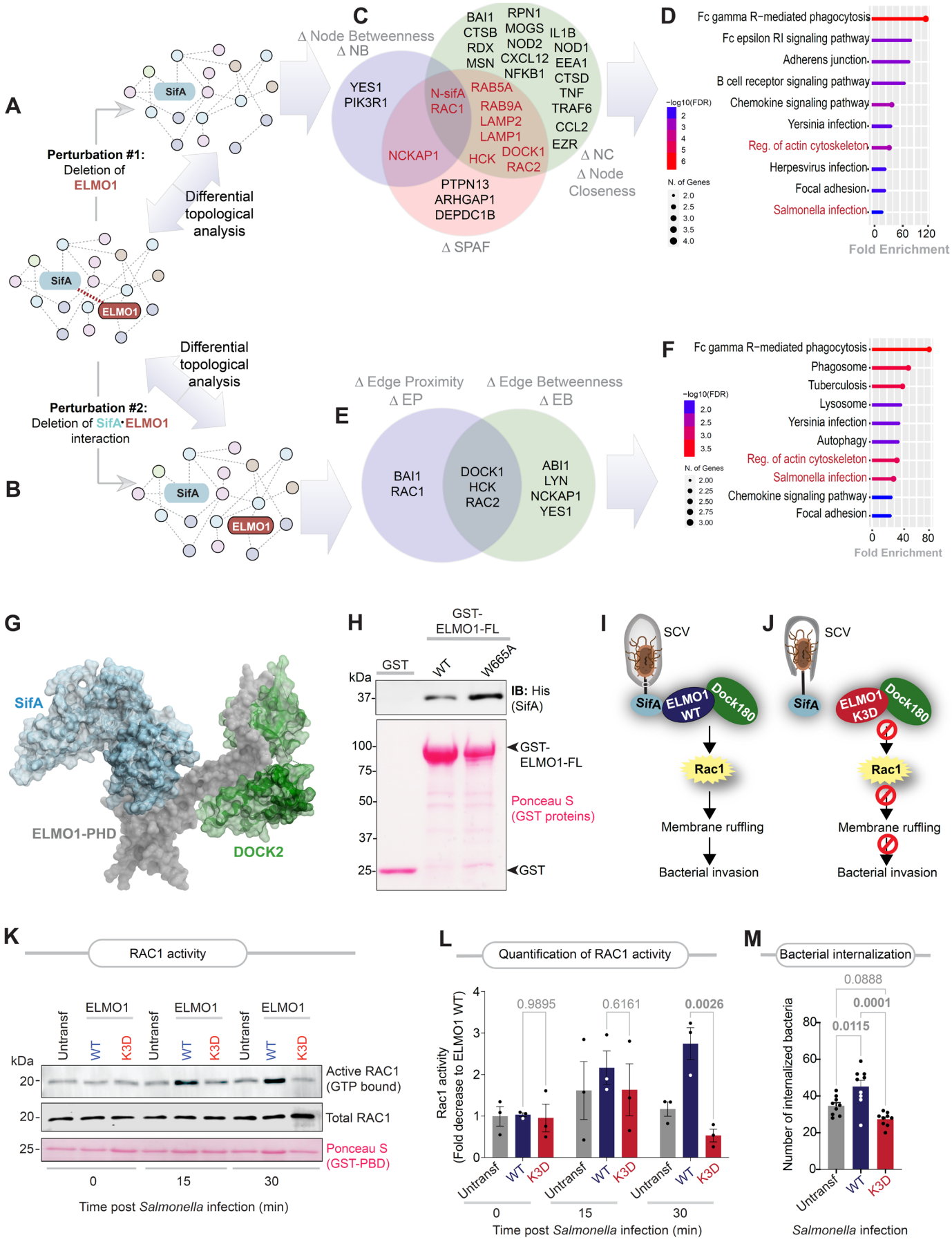

Figure 3. Prediction and validation of the consequences of disruption of the ELMO1•SifA interface.

A-B. A SifA (*Salmonella*)•human PPI network was constructed using a previously identified BioID-determined interactome of SifA [27] and their connectors were fetched from the human STRING database [39]. Network perturbation was carried out *in-silico* either by deletion of ELMO1 (A; node deletion) or selective disruption of the ELMO1•SifA interaction (B; edge deletion).

C-D. Venn-diagram (C) shows sets of proteins that were impacted by *in-silico* deletion of ELMO1, as determined by three independent metrics of network topological analyses: differential node betweenness (ΔNB), node closeness (ΔNB) and shortest path alteration fraction (ΔSPAF). Lollipop plots (D) indicate the KEGG pathways enriched among the proteins that were identified as impacted based on more than one node-based metric. See **Supplementary Figure 3** for a detailed analysis.

E-F. Venn-diagram (E) shows sets of proteins that were impacted by *in-silico* deletion of the ELMO1•SifA interaction, as determined by two metrics of network topological analyses: differential edge betweenness (ΔEB) and edge proximity (ΔEP). Lollipop plots (F) indicate the KEGG pathways enriched among the proteins that were identified using edge-based metrices. See **Supplemental Information 1** for a detailed list of nodes and edges.

G. A homology model of a co-complex between SifA (light blue), ELMO1 (gray), and DOCK180 (green), built by overlaying resolved crystal structures of DOCK2•ELMO1 (PDB:3A98)[18], ELMO1 (PDB:2VSZ) and SifA•SKIP (PDB:3CXB).

H. Recombinant His-SifA (~5ug) were used in a GST pulldown assay with GST (negative control), and GST-tagged wild-type (WT) and W665A mutants of full length (FL) ELMO1, and bound SifA was visualized by immunoblot using anti-His (SifA) antibody. Equal loading of GST proteins is confirmed by Ponceau S staining.

I-J: Key steps in SifA•ELMO1•Dock180 co-complex mediated Rac1 signaling (I) and the predicted impact of selectively disrupting SifA•ELMO1 interaction using the K3D mutant (J) are shown.

K-L. ELMO1-depleted J774 macrophages (Untransfected) transfected with either WT or K3D mutant ELMO1 and subsequently infected with *Salmonella* (MOI 10; at indicated time points post-infection) were assessed for Rac1 activation by pulldown assays using GST-PBD. Immunoblots and Ponceau S-stained GST proteins are shown in K. Quantification of immunoblots in L. Results are displayed as mean ± S.E.M (n = 3 independent replicates). Statistical significance was determined using one-way ANOVA.

M: Bar graph represents the number of internalized bacteria by the same cells in K infected with *Salmonella* (MOI 10; 30 min post-infection). Results are displayed as mean ± S.E.M (n = 3 independent replicates). Statistical significance was determined using one-way ANOVA.

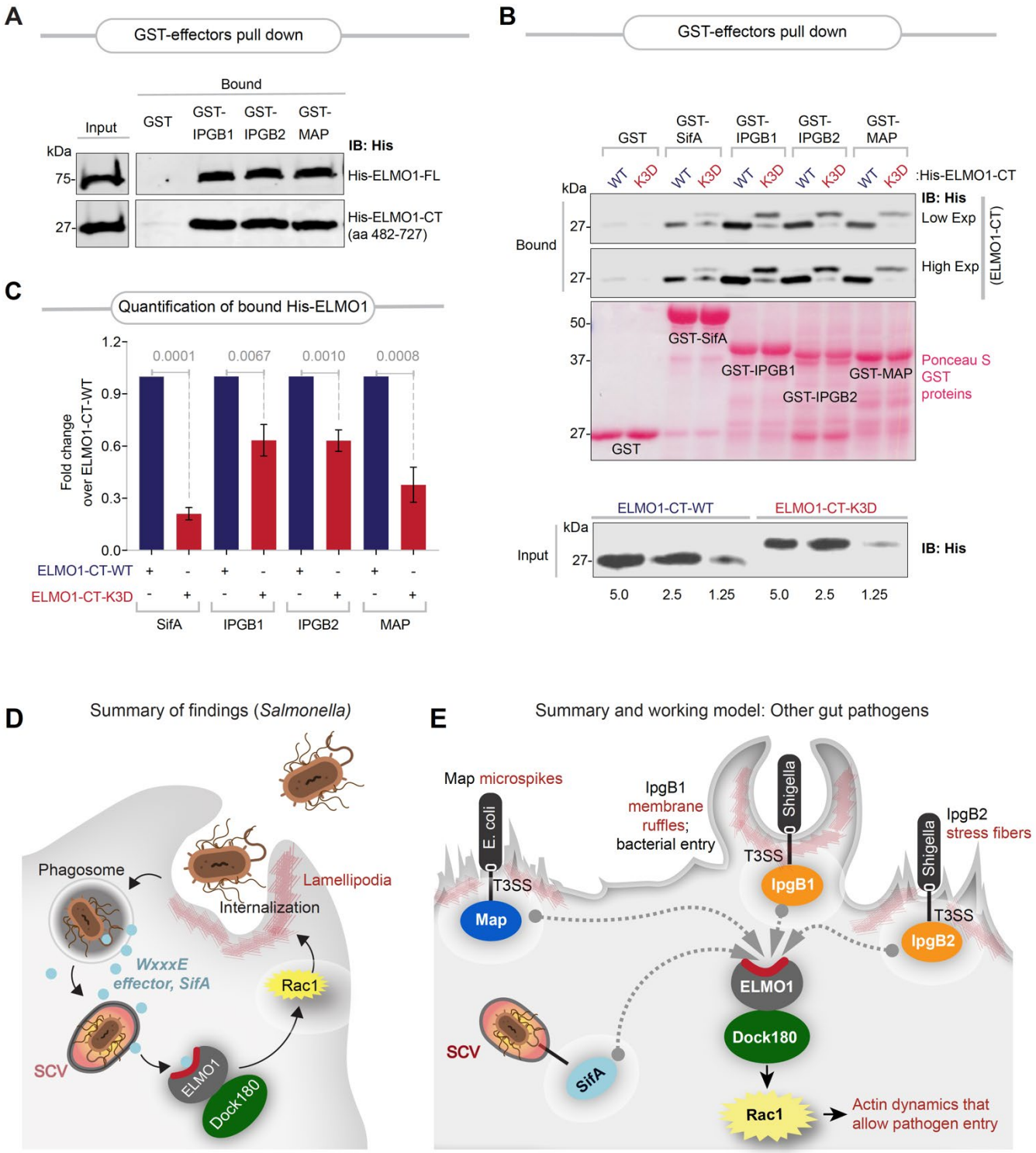

Figure 4: The SifA•ELMO1 interface is a conserved site for engaging diverse WxxxE-effectors.

A. Recombinant His-tagged CT (aa 482-727) or full-length (FL) ELMO1 proteins (~3 µg) were used in a pulldown assay with immobilized full-length GST-tagged WxxxE effectors (SifA, IpgB1, IpgB2, Map) or GST alone (negative control). Bound ELMO1 proteins were visualized by immunoblot using anti-His (SifA) antibody. GST proteins are visualized by Ponceau S staining.

B. Recombinant WT or K3D mutant His-ELMO1-CT proteins (~3 µg) were used in pulldown assays with immobilized GST-tagged full-length effectors as in A. Bound ELMO1 was visualized by immunoblotting using an anti-His antibody. GST proteins are visualized by Ponceau S staining.

C. Quantification of immunoblots in B. Results are displayed as mean ± S.E.M (n = 3 independent replicates). Statistical significance was determined using an unpaired t-test.

D-E. Schematic (D) summarizes the key findings in this work using *Salmonella* and its WxxxE-motif effector, SifA. Schematic (E) summarizes the key biochemical findings and the working model proposed for how diverse microbes use their *WxxxE* motif-containing virulence factors (effectors) to hijack the host engulfment pathway via a shared mechanism. Although diverse in sequence (see **Supplementary Figure 4** for an alignment of WxxxE effectors) and function, they all bind a conserved surface on ELMO1 (highlighted in red). The major consequence of such WxxxE-effector•ELMO1 interaction is enhanced Rac1 activation and bacterial engulfment.

STAR METHODS

KEY RESOURCES TABLE

REAGENT or RESOURCE	SOURCE	IDENTIFIER
Antibodies		
Mouse monoclonal anti-poly-His	Sigma-Aldrich	Cat# H1029
Mouse mononclonal anti-FLAG	Cell Signaling	Cat# 8146S
Mouse monoclonal ELMO1 antibody	Santa Cruz Biotechnology	Cat# sc-271519
IRDye 800CW Goat anti-Mouse IgG Secondary	LI-COR Biosciences	Cat# 926-32210
IRDye 680RD Goat anti-Rabbit IgG Secondary	LI-COR Biosciences	Cat# 926-68071
Biological samples		
HEK 293	ATCC	CRL-1573
sh Control J774 and sh ELMO1 J774 murine macrophage cell lines	Sayed et al., 2021[20]	n/a
Salmonella enteric serovar Typhimurium (strain SL1344)	ATCC	Cat#700720
SifA mutant strain	Obtained from Olivia Steele-Mortimer (NIH/NIAID)	n/a
Chemicals, peptides		
HisPurâ Cobalt Resin	Thermo Scientific	Cat# 89964
Glutathione Sepharoseâ 4B	Sigma-Aldrich	Cat# GE17-0756-04
PVDF Transfer Membrane, 0.45mM	Thermo Scientific	Cat# 88518
Polyethylenimine (PEI)	Polysciences	Cat# Inc 23966
Protease inhibitor cocktail	Roche	Cat# 11 873 580 001
Critical commercial assay kits		
Rac1 Pull-Down Activation Assay Biochem Kit (Bead Pull-Down Format)	Cytoskeleton.Inc.	Cat# BK035-S
Plasmids and recombinant proteins		
pGEX-6P-2 (GST)	GE Healthcare	Cat# 28-9546-50
GST ELMO1 full-length (FL)	Sayed et al., 2021[20]	n/a
GST ELMO1 CT (aa 482-727)	*This paper*	n/a
GST SifA WT	Sayed et al., 2021[20]	n/a
GST SifA L130D	*This paper*	n/a
GST-IPGB1	*This paper*	Cloned from FLAG-IPGB1 provided by Neil Alto, UT Dallas
GST-IPGB2	*This paper*	Cloned from FLAG-IPGB2 provided by Neil Alto, UT Dallas
GST- MAP	*This paper*	Cloned from FLAG-Map provided by Neil Alto, UT Dallas
pET-28a (His)	Novagene	Cat# 69864
His ELMO1 full-length (FL)	*This paper*	n/a
His ELMO1 CT (aa 482-727)	*This paper*	n/a
His ELMO1 K620D/K626D/K628D	*This paper*	n/a
His SifA WT	*This paper*	n/a
His SifA L130D	*This paper*	n/a
His SifA M131D	*This paper*	n/a
His SifA L130D/M131D	*This paper*	n/a
FLAG ELMO1 (WT)	Sayed et al., 2021[20]	n/a
FLAG ELMO1 (K3D)	*This paper*	K620D; K626D; K628D

Mutagenesis Primers	Forward primer	Reverse primer
Mouse ELMO1 K620D/K626D/K628D	5'-tgttttgtttaagggcaccatcctcatccatatgaggcagtcctttcccgtc-3' 5'-gacgggaaaggactgccctcatatggatgaggatggtgcccttaaacaaaaca-3' 5'-caaagcagtggtgacgggagatgactgccctcatatgaaag-3'	5'-ctttcatatgagggcagtcatctcccgtcaccactgctttg-3'
SifA L130D	5'-ccgggcgatctttcatatcaaaataaagattccccatgacttcacagct-3'	5'-agctgtgaagtcatggggaatctttattttgatatgaaagatcgcccgg-3'
SifA M131D	5'-ttaaaatatccgggcgatctttatcatcaaaataaagattccccatgacttcacagc-3'	5'-gctgtgaagtcatggggaatctttattttgatgataaagatcgcccggatattttaa-3'
Cloning Primers	**Forward primer (5'→3')**	**Reverse primer (5'→3')**
Elmo1FL		
Elmo1 CT (BamHI/Not1)	cgcggatccatgcaggtggtgaaggagcagg	gcgacgcggccgctgttacagtcatagacaaagtcatagttgctaggttcct
IPGB1 (KpnI/BamHI)	catggtaccatgcaaattctaaacaaaatacttccacaggt	cgcggatccttaatttgtattgctttgacggtatacagcctt
IPGB2 (KpnI/BamHI)	catggtaccatgcttggaacatcttttaataattttggaatcagt	cgcggatcctcagaaaggcgattctaaatttgtaatatagtcac
MAP (EcoRI/KpnI)	ccggaattccatgtttagtccaatgacaatggcagg	catggtaccctacaatcgggtatcctgtacatgctc
Software and algorithms		
ImageStudio Lite	LI-COR	https://www.licor.com/bio/image-studio-lite/
Prism	GraphPad	Home - GraphPad
PyMOL Molecular Graphics System		https://pymol.org/2
ShinyGO v0.76		http://bioinformatics.sdstate.edu/go/
Codes for the construction and analysis of the PPI networks		https://github.com/sinha7290/ELMO
Publicly deposited structures and/or datasets		
ELMO1 (PH domain)	PDB:2VSZ	https://www.rcsb.org/structure/2VSZ
SKIP-PH bound to SifA	PDB:3CXB	https://www.rcsb.org/structure/3CXB
DOCK2-bound to ELMO1	PDB:3A98	https://www.rcsb.org/structure/3A98
Proximity ligation assay (BioID)	SifA interactome	D'Costa VM et al.,[27]

RESOURCE AVAILABILITY

LEAD CONTACT

Further information and requests for resources and reagents should be directed to and will be fulfilled by the lead contact, Pradipta Ghosh, prghosh@ucsd.edu.

MATERIALS AVAILABILITY

This study has generated constructs and cell lines. These materials can only be accessed through proper material transfer agreement following the guidelines of the University of California, San Diego.

DATA AND CODE AVAILABILITY

- All data is available in the main text or the supplementary materials. Original western blot images and microscopy data will be shared by the lead contact upon request. This paper also analyzes an existing, publicly available proteomics dataset and protein structures (listed in the Key Resources Table). Source data for gene ontology analyses are provided with this paper.
- This paper includes PPI network analysis; a link to the codes is provided (**Key Resources Table**)
- Any additional information required to reanalyze the data reported in this paper is available from the lead contact upon request.

CONFLICT OF INTEREST STATEMENT: All authors declare no conflicts of interests, financial or non-financial in nature, or connections, direct or indirect or other situations that might raise the question of bias in the work reported or the conclusions, implications, or opinions stated here– including pertinent commercial or other sources of funding.

EXPERIMENTAL MODEL AND SUBJECT DETAILS

J774 macrophage and human (HEK) cell lines were used in various assays. Bacterial strains were used to infect macrophages in various experiments. This study does not involve the use of human subjects or animals.

METHOD DETAILS

Plasmid constructs and mutagenesis.

ELMO1 and SifA (from SL1344) were amplified by PCR and cloned into pET-28a (+) and pGEX-6P-2 plasmid vectors to generate His- and GST-tagged proteins, respectively. ELMO1 CT (aa 482-727) was amplified by PCR from human ELMO1 cDNA (Clone IRAUp969C0316D, SourceBioscience Inc) and subcloned into pET-28a (+) and pGEX-6P-2 plasmid vectors using BamHI and NotI restriction sites. Effector proteins IPGB1,

IPGB2 and MAP were amplified from FLAG-tagged effector constructs (obtained from Neil Alto, UT Dallas) and cloned into pGEX-6P-2 plasmid vectors. ELMO1 and SifA mutations were generated by site directed mutagenesis using the Quick-Change II Site-Directed Mutagenesis kit (Agilent Technologies) and specific primers (**Key Resource Table**) according to manufacturer's protocol. All plasmid constructs and mutagenesis were verified by sequencing and protein expression was verified by western blot analysis.

Bacteria and bacterial culture

Salmonella enterica serovar *Typhimurium* strain SL1344, were obtained from the American Type Culture Collection (ATCC) (Manassas, VA, USA), and SL1344 Δ*SifA* mutant strain was obtained from Olivia Steele Mortimer (NIH/NIAID)[40,41] . The bacterial strains were propagated as described previously [42,43]. Briefly, a single colony was inoculated into LB broth and grown for 8 h under aerobic conditions and then under oxygen-limiting conditions. For SL1344 Δ*SifA* mutant strain, streptomycin with final conc (100 µg/mL) was added to LB broth. Cells were infected with a multiplicity of infection (moi) of 10.

Cell culture and transfection

HEK cells were obtained from American Type Culture Collection, (Manassas, VA, USA). Control and ELMO1 depleted shRNA J774 cells were generated as previously described [44]. Cells were maintained in high glucose DMEM (Life Technologies) containing 10% fetal bovine serum and 100 U/ml penicillin and streptomycin at 37ºC in a 5% CO2 incubator. Cells were sub-cultured 24 h prior to transfection. Transfections of plasmids were performed using Lipofectamine 2000 (Invitrogen) according to manufacturer's protocol.

Transmission electron microscopy (TEM)

Control (shControl) and ELMO1-depleted (shELMO1) J477 macrophages were infected with *Salmonella* enterica serovar *Typhimurium* strain SL1344 (SL) and its mutant strain *SifA* [MOI 30] and the infected pellets were fixed with Glutaraldehyde in 0.1 M Sodium Cacodylate Buffer, (pH 7.4) followed by post-fixation with 1% OsO4 in 0.1 M cacodylate buffer for 1 h on ice followed by staining with 2% uranyl acetate for 1 h and dehydrated in ethanol (50-100%) on ice. The cells were washed for 10 min each once with 100% ethanol and two times with acetone and embedded with Durcupan. A Leica UCT ultramicrotome was used to section 60 nm cuts and picked up on 300 mesh copper grids. Sections were post-stained first with 2% uranyl acetate (5 min) and Sato's lead stain (1 min) prior to visualization using a JEOL-1400plus equipped with a bottom-mount Gatan (4k x 4k) camera.

Protein expression and purification

Recombinant His and GST-tagged proteins were expressed in Escherichia coli strain BL21 (DE3) and purified as previously described (1, 2). Briefly, proteins in bacterial culture were induced with IPTG (1 mM) overnight incubation at 25°C. Centrifuged and cell pellet were then lysed in either GST lysis buffer containing 25 mM Tris-HCl (pH 7.4) 20 mM NaCl, 1 mM EDTA, 20% (v/v) glycerol, 1% (v/v) Triton X-100, protease inhibitor cocktail or His lysis buffer containing 50 mM NaH_2PO_4 (pH 7.4), 300 mM NaCl, 10 mM imidazole, 1% (v/v) Triton-X-100, protease inhibitor cocktail and then sonicated briefly to ensure better lysis. Cell lysate were centrifugation at 12,000 x g at 4°C for 30 mins to remove cell debris. Cleared cell lysate was then affinity

purified using either glutathione-Sepharose 4B beads or HisPur Cobalt Resin, followed by elution and overnight dialysis in PBS. Proteins were aliquoted and stored at -80°C prior to use.

GST pulldown assays

Recombinant purified GST-tagged proteins were immobilized onto glutathione-Sepharose beads in a binding buffer containing 50 mM Tris-HCl (pH 7.4), 100 mM NaCl, 0.4% (v/v) Nonidet P-40, 10 mM $MgCl_2$, 5 mM EDTA, 2 mM DTT for 60 min at 4°C. GST-tagged protein bound beads were washed and incubated with purified His-tagged proteins in a binding buffer for 4 h at 4°C. Protein bound complexes on a beads were washed four times with phosphate wash buffer containing 4.3 mM Na_2HPO_4, 1.4 mM KH_2PO_4 (pH 7.4), 137 mM NaCl, 2.7 mM KCl, 0.1% (v/v) Tween-20, 10 mM $MgCl_2$, 5 mM EDTA, 2 mM DTT, 0.5 mM sodium orthovanadate and eluted by boiling beads in reducing sample buffer containing 5% SDS, 156 mM Tris-Base, 25% glycerol, 0.025% bromophenol blue, 25% β-mercaptoethanol. Bound proteins and lysates were fractionated by SDS/PAGE gel and analyzed by immunoblot.

Quantitative immunoblotting

For immunoblotting, protein samples were separated by 10% SDS-PAGE and transferred to polyvinylidene fluoride (PVDF) membranes. Membranes were blocked with 5% non-fat milk in Tris-buffered saline with 0.1% Tween® 20 detergent (1X TBST). The membrane was stained with Ponceau S to visualize bait proteins (GST), washed, blocked (5% milk), and incubated with primary antibody solutions overnight at 4°C (unless otherwise specified, a 1:500 dilution for primary antibody was used). Washed blots were then incubated with infrared secondary antibodies (see Key Resource Table) for 1 h at room temperature. Dual color infrared imaging and quantifications of immunoblots were performed using a Li-Cor Odyssey imaging system and analyzed using the Image StudioLite software as per manufacturer's instructions.

Homology modelling and protein docking

For the structure-guided mutagenesis studies, we took into consideration the following three previously resolved structures, all accessed through the Protein Data Bank (PDB; https://www.rcsb.org/)-- (i) PDB:3CXB, a 2.60 Å resolved crystal structure of the PH domain of SKIP (3CXB, golden brown) in complex with full length SifA (3CXB, cyan; (ii) PDB:2VSZ, a 2.30 Å resolved crystal structure of the C-terminal 200 aa (containing the PH domain) of ELMO1 in complex with the N-terminal 200 aa of DOCK180; (iii) PDB:3A98, a 2.10 N-terminal 177 aa fragment of DOCK2 and the C-terminal 196 aa fragment (containing the PH domain) of ELMO1. First, the PH domain of SKIP (PDB:3CXB; template) was superimposed to the PH-domain of ELMO1 (PDB:2VSZ). The performed analysis of the PH domains revealed them to be quite similar in structure SKIP and ELMO1 (RMSD of 1.528). Subsequently, the PH domain was used for molecular docking with SifA. Protein docking and the prediction of the contact sites at the ELMO1•SifA interface was performed by using HADDOCK (High Ambiguity Driven protein−protein Docking) web server and the final representation was using Pymol visualization tool (https://pymol.org/2/) The PyMOL Molecular Graphics System. Delano Scientific, San Carlos). The HADDOCK server was run using default parameters and the top 10 predicted

models were further reanalyzed for checking the polar contacts. The best fit protein model was used for our prediction of the protein binding interface.

Construction, perturbation, and analysis of the Protein-Protein Interaction Network

A SifA (*Salmonella*)•human interaction network was constructed using a previously identified BioID-determined interactome of SifA [39] and their connectors, fetched from the human STRING database [45,46]. To avoid false positive interactions, a Stepminer-derived cutoff of combined interaction score was selected [45,46]. A complete list of edges is provided in **Supplemental Information 1**.

Once constructed, the network was perturbed using two approaches. First, an *in-silico* deletion of ELMO1 was performed, and each node within this perturbed network (without ELMO1) was assessed for the following network metrics: (i) Betweenness centrality, (ii) Closeness centrality, and (iii) Shortest Path Alteration Fraction (SPAF) [47]. Difference in Z score, ΔZ, of each node, N, for each of the above mentioned topological metrices was calculated. Proteins with $\Delta Z > 0.1$ were identified as those that were impacted due to the deletion of ELMO1.

As a second approach, an *in-silico* deletion of ELMO1•SifA interaction(edge) was performed, and each edge within this perturbed network (without ELMO1•SifA edge) was assessed for two independent metrices: (i) Edge betweenness centrality and (ii) Edge Proximity [48]. Edges with $\Delta Z > 0.1$ were identified as those that were impacted due to the selective deletion of the ELMO1•SifA interaction.

A group of proteins that are impacted, as determined by at least more than one topological node-based metrices, or either of the two edge-based metrics, were used for KEGG enrichment analysis (using ShinyGO v0.76; http://bioinformatics.sdstate.edu/go/). All the codes for network analysis are available at https://github.com/sinha7290/ELMO.

Measurement of Rac1 activity

ELMO1-depleted murine J774 macrophage cell lines were transfected with ELMO1 WT and ELMO1 K3D plasmids and infected with *Salmonella enterica* serovar Typhimurium for 15 and 30 min (MOI 1:50) and Rac1 activity was measured by pull-down assay using a commercial kit. First, infected cells were lysed with the lysis buffer provided in the kit. Equal aliquots of cell lysates (~ 800 µg total cell protein) were added to 10 µg (10 µl) of immobilized GST-PBD (glutathione *S*-transferase with p21-binding domain of Pak1) (a.k.a., PAK-PBD beads) and incubated at 4°C on a rotator for 1 h. PAK-PBD beads were recovered by centrifugation at 5,000 x g at 4°C. Unbound lysates were removed and the beads were washed once with 500 µl Wash Buffer prior to eluting the proteins with 20 µl of 2x Laemmli sample buffer and boiling for 5 min at 100°C. Input lysates and eluates from the PAK-PBD beads were resolved on a 12.5% SDS-PAGE, and transferred for 45 min, followed by quantitative immunoblotting.

Bacterial internalization assays

Approximately $0.5*10^6$ ELMO1-depleted murine macrophage cells were seeded into 12-well culture dishes ~12 h before transfection with either FLAG-ELMO1 WT or FLAG-ELMO1 K3D. After 48 hours of transfection, cells were infected with SL at a MOI of 1:50 for 30 min in antibiotic free media. The cells were then washed

and incubated with gentamicin (500 mg/ml) for 90 min to kill the extracellular bacteria. Subsequently, the cells were lysed in 1% Triton-X100, and the lysates were serially diluted and plated directly onto Luria-Bertani agar plates. The total colony-forming units (CFUs) were enumerated the next day after overnight incubation of the plates at 37°C.

Image Processing

All images were processed on ImageJ software (NIH) or iStudio (LiCOR) software and assembled into figure panels using Photoshop and Illustrator (Adobe Creative Cloud). All graphs were generated using GraphPad Prism v9.3.1.

QUANTIFICATION AND STATISTICAL ANALYSIS

Statistical Analysis and Replicates

All experiments were repeated at least three times, and results were presented as average ± S.E.M. Statistical significance was assessed using either t-test or one-way analysis of variance (ANOVA) including a Tukey's test for multiple comparisons. Actual *p* values are displayed.

ACKNOWLEDGEMENTS

We thank Soumita Das (UC San Diego, CA; currently at University of Massachusetts, Lowell, MA) for numerous reagents and constructs that were used in this work and for helpful discussions. This work was supported by the National Institute of Health (NIH) Grants: R01-AI141630, UG3TR003355, UG3TR002968 and R01-AI55696 (P.G). PG was also supported by the Leona M. and Harry B. Helmsley Charitable Trust and NIH programs. G.D.K. was supported through The American Association of Immunologists (AAI) Intersect Fellowship Program for Computational Scientists and Immunologists. S.R was supported, in part, by the NIH grants (AI118985 and GM117424) and M.A was supported by R01-DK107585 and R01-AI141630. S.R.I was supported by a NIH Diversity Supplement award (3R01DK107585-02S1). We thank Ying Jones (UC San Diego Electron Microscopy Core Facility) for technical and logistical support. The content is solely the responsibility of the authors and does not necessarily represent the official views of the Helmsley Charitable Trust or the National Institutes of Health.

AUTHOR CONTRIBUTIONS

M. A., and P.G designed, executed, and analyzed most of the experiments and/or formal analysis in this work. M.A carried out all the biochemical and functional assays. M.A and G.K carried out semi-quantitative transmission-electron microscopy (TEM). A.B and S. R generated and analyzed the sequence and structure homology models. S. S. created and analyzed the PPI networks. S.R.C generated the mutant constructs. H.G and A.A provided technical assistance for bacterial clearance studies. G.K and P.G prepared and/or created display items for data visualization and/or presentation. M.A, G.K. and P.G wrote the manuscript. All authors reviewed and edited the manuscript and approved its final version.

Inclusion and diversity

One or more of the authors of this paper belongs to a minority group underrepresented in science.

REFERENCES

1 Steele-Mortimer, O. The Salmonella-containing vacuole: moving with the times. *Curr Opin Microbiol* **11**, 38-45, doi:10.1016/j.mib.2008.01.002 (2008).

2 Castanheira, S. & García-Del Portillo, F. Salmonella Populations inside Host Cells. *Front Cell Infect Microbiol* **7**, 432, doi:10.3389/fcimb.2017.00432 (2017).

3 Lai, Y., Rosenshine, I., Leong, J. M. & Frankel, G. Intimate host attachment: enteropathogenic and enterohaemorrhagic Escherichia coli. *Cell Microbiol* **15**, 1796-1808, doi:10.1111/cmi.12179 (2013).

4 Smith, K., Humphreys, D., Hume, P. J. & Koronakis, V. Enteropathogenic Escherichia coli recruits the cellular inositol phosphatase SHIP2 to regulate actin-pedestal formation. *Cell Host Microbe* **7**, 13-24, doi:10.1016/j.chom.2009.12.004 (2010).

5 Watson, J. L. *et al.* Shigella sonnei O-Antigen Inhibits Internalization, Vacuole Escape, and Inflammasome Activation. *mBio* **10**, doi:10.1128/mBio.02654-19 (2019).

6 Handa, Y. *et al.* Shigella IpgB1 promotes bacterial entry through the ELMO-Dock180 machinery. *Nat Cell Biol* **9**, 121-128, doi:10.1038/ncb1526 (2007).

7 Finlay, B. B. & Cossart, P. Exploitation of mammalian host cell functions by bacterial pathogens. *Science* **276**, 718-725, doi:10.1126/science.276.5313.718 (1997).

8 Galán, J. E. & Collmer, A. Type III secretion machines: bacterial devices for protein delivery into host cells. *Science* **284**, 1322-1328, doi:10.1126/science.284.5418.1322 (1999).

9 Cossart, P. & Sansonetti, P. J. Bacterial invasion: the paradigms of enteroinvasive pathogens. *Science* **304**, 242-248, doi:10.1126/science.1090124 (2004).

10 Connor, M. G. *et al.* Yersinia pestis Targets the Host Endosome Recycling Pathway during the Biogenesis of the Yersinia-Containing Vacuole To Avoid Killing by Macrophages. *mBio* **9**, doi:10.1128/mBio.01800-17 (2018).

11 Watson, R. O. & Galán, J. E. Campylobacter jejuni survives within epithelial cells by avoiding delivery to lysosomes. *PLoS Pathog* **4**, e14, doi:10.1371/journal.ppat.0040014 (2008).

12 Coburn, B., Sekirov, I. & Finlay, B. B. Type III secretion systems and disease. *Clin Microbiol Rev* **20**, 535-549, doi:10.1128/cmr.00013-07 (2007).

13 Orchard, R. C. *et al.* Identification of F-actin as the dynamic hub in a microbial-induced GTPase polarity circuit. *Cell* **148**, 803-815, doi:10.1016/j.cell.2011.11.063 (2012).

14 Alto, N. M. *et al.* Identification of a bacterial type III effector family with G protein mimicry functions. *Cell* **124**, 133-145, doi:10.1016/j.cell.2005.10.031 (2006).

15 Sayed, I. M. *et al.* The interaction of enteric bacterial effectors with the host engulfment pathway control innate immune responses. *Gut Microbes* **13**, 1991776, doi:10.1080/19490976.2021.1991776 (2021).

16 Xue, R. *et al.* Functional Verification of Novel ELMO1 Variants by Live Imaging in Zebrafish. *Front Cell Dev Biol* **9**, 723804, doi:10.3389/fcell.2021.723804 (2021).

17 Grimsley, C. M. *et al.* Dock180 and ELMO1 proteins cooperate to promote evolutionarily conserved Rac-dependent cell migration. *J Biol Chem* **279**, 6087-6097, doi:10.1074/jbc.M307087200 (2004).

18 Hanawa-Suetsugu, K. *et al.* Structural basis for mutual relief of the Rac guanine nucleotide exchange factor DOCK2 and its partner ELMO1 from their autoinhibited forms. *Proc Natl Acad Sci U S A* **109**, 3305-3310, doi:10.1073/pnas.1113512109 (2012).

19 Kukimoto-Niino, M., Ihara, K., Murayama, K. & Shirouzu, M. Structural insights into the small GTPase specificity of the DOCK guanine nucleotide exchange factors. *Curr Opin Struct Biol* **71**, 249-258, doi:10.1016/j.sbi.2021.08.001 (2021).

20 Das, S. *et al.* ELMO1 has an essential role in the internalization of Salmonella Typhimurium into enteric macrophages that impacts disease outcome. *Cell Mol Gastroenterol Hepatol* **1**, 311-324, doi:10.1016/j.jcmgh.2015.02.003 (2015).

21 Ruiz-Albert, J. *et al.* Complementary activities of SseJ and SifA regulate dynamics of the Salmonella typhimurium vacuolar membrane. *Mol Microbiol* **44**, 645-661, doi:10.1046/j.1365-2958.2002.02912.x (2002).

22 Beuzón, C. R. *et al.* Salmonella maintains the integrity of its intracellular vacuole through the action of SifA. *Embo j* **19**, 3235-3249, doi:10.1093/emboj/19.13.3235 (2000).

23 Ohlson, M. B. *et al.* Structure and function of Salmonella SifA indicate that its interactions with SKIP, SseJ, and RhoA family GTPases induce endosomal tubulation. *Cell Host Microbe* **4**, 434-446, doi:10.1016/j.chom.2008.08.012 (2008).

24 Arpaia, N. *et al.* TLR signaling is required for Salmonella typhimurium virulence. *Cell* **144**, 675-688, doi:10.1016/j.cell.2011.01.031 (2011).

25 Dumont, A. *et al.* SKIP, the host target of the Salmonella virulence factor SifA, promotes kinesin-1-dependent vacuolar membrane exchanges. *Traffic* **11**, 899-911, doi:10.1111/j.1600-0854.2010.01069.x (2010).
26 Diacovich, L. *et al.* Interaction between the SifA virulence factor and its host target SKIP is essential for Salmonella pathogenesis. *J Biol Chem* **284**, 33151-33160, doi:10.1074/jbc.M109.034975 (2009).
27 D'Costa, V. M. *et al.* BioID screen of Salmonella type 3 secreted effectors reveals host factors involved in vacuole positioning and stability during infection. *Nat Microbiol* **4**, 2511-2522, doi:10.1038/s41564-019-0580-9 (2019).
28 Sarkar, A. *et al.* ELMO1 Regulates Autophagy Induction and Bacterial Clearance During Enteric Infection. *J Infect Dis* **216**, 1655-1666, doi:10.1093/infdis/jix528 (2017).
29 Sayed, I. M. *et al.* Host engulfment pathway controls inflammation in inflammatory bowel disease. *Febs j* **287**, 3967-3988, doi:10.1111/febs.15236 (2020).
30 Makino, Y. *et al.* Tyr724 phosphorylation of ELMO1 by Src is involved in cell spreading and migration via Rac1 activation. *Cell Commun Signal* **13**, 35, doi:10.1186/s12964-015-0113-y (2015).
31 Yokoyama, N. *et al.* Identification of tyrosine residues on ELMO1 that are phosphorylated by the Src-family kinase Hck. *Biochemistry* **44**, 8841-8849, doi:10.1021/bi0500832 (2005).
32 Kukimoto-Niino, M. *et al.* Cryo-EM structure of the human ELMO1-DOCK5-Rac1 complex. *Sci Adv* **7**, doi:10.1126/sciadv.abg3147 (2021).
33 Lu, M. *et al.* PH domain of ELMO functions in trans to regulate Rac activation via Dock180. *Nat Struct Mol Biol* **11**, 756-762, doi:10.1038/nsmb800 (2004).
34 Li, Y., Huang, Y., Swaminathan, C. P., Smith-Gill, S. J. & Mariuzza, R. A. Magnitude of the hydrophobic effect at central versus peripheral sites in protein-protein interfaces. *Structure* **13**, 297-307, doi:10.1016/j.str.2004.12.012 (2005).
35 Ambler, R. P. & Rees, M. W. Epsilon-N-Methyl-lysine in bacterial flagellar protein. *Nature* **184**, 56-57, doi:10.1038/184056b0 (1959).
36 Huang, J. *et al.* p53 is regulated by the lysine demethylase LSD1. *Nature* **449**, 105-108, doi:10.1038/nature06092 (2007).
37 Makino, Y. *et al.* Elmo1 inhibits ubiquitylation of Dock180. *J Cell Sci* **119**, 923-932, doi:10.1242/jcs.02797 (2006).
38 Song, J. H. *et al.* TLR4 activation induces inflammatory vascular permeability via Dock1 targeting and NOX4 upregulation. *Biochim Biophys Acta Mol Basis Dis* **1868**, 166562, doi:10.1016/j.bbadis.2022.166562 (2022).
39 Szklarczyk, D. *et al.* The STRING database in 2021: customizable protein-protein networks, and functional characterization of user-uploaded gene/measurement sets. *Nucleic Acids Res* **49**, D605-D612, doi:10.1093/nar/gkaa1074 (2021).
40 Steele-Mortimer, O. *et al.* The invasion-associated type III secretion system of Salmonella enterica serovar Typhimurium is necessary for intracellular proliferation and vacuole biogenesis in epithelial cells. *Cell Microbiol* **4**, 43-54, doi:10.1046/j.1462-5822.2002.00170.x (2002).
41 Stein, M. A., Leung, K. Y., Zwick, M., Garcia-del Portillo, F. & Finlay, B. B. Identification of a Salmonella virulence gene required for formation of filamentous structures containing lysosomal membrane glycoproteins within epithelial cells. *Mol Microbiol* **20**, 151-164, doi:10.1111/j.1365-2958.1996.tb02497.x (1996).
42 Das, S. *et al.* ELMO1 has an essential role in the internalization of Typhimurium into enteric macrophages that impacts disease outcome. *Cell Mol Gastroenterol Hepatol* **1**, 311-324, doi:10.1016/j.jcmgh.2015.02.003 (2015).
43 den Hartog, G. *et al.* Apurinic/Apyrimidinic Endonuclease 1 Restricts the Internalization of Bacteria Into Human Intestinal Epithelial Cells Through the Inhibition of Rac1. *Front Immunol* **11**, 553994-553994, doi:10.3389/fimmu.2020.553994 (2021).
44 Das, S. *et al.* Brain angiogenesis inhibitor 1 (BAI1) is a pattern recognition receptor that mediates macrophage binding and engulfment of Gram-negative bacteria. *Proceedings of the National Academy of Sciences of the United States of America* **108**, 2136-2141, doi:10.1073/pnas.1014775108 (2011).
45 Sahoo, D. *et al.* MiDReG: a method of mining developmentally regulated genes using Boolean implications. *Proc Natl Acad Sci U S A* **107**, 5732-5737, doi:10.1073/pnas.0913635107 (2010).
46 Qiao, L. *et al.* A circuit for secretion-coupled cellular autonomy in multicellular eukaryotic cells. *Mol Syst Biol*, e11127, doi:10.15252/msb.202211127 (2023).
47 Sinha, S., Samaddar, S., Das Gupta, S. K. & Roy, S. Network approach to mutagenesis sheds insight on phage resistance in mycobacteria. *Bioinformatics*, doi:10.1093/bioinformatics/btaa1103 (2021).

48 Banerjee, S. J., Sinha, S. & Roy, S. Slow poisoning and destruction of networks: edge proximity and its implications for biological and infrastructure networks. *Phys Rev E Stat Nonlin Soft Matter Phys* **91**, 022807, doi:10.1103/PhysRevE.91.022807 (2015).